it is nevertheless interesting to note that in the region of 0.55 Ry (i.e., near the free-electron Fermi energy) the values of A_l are rather close to unity. In the spirit of Lee and Heine's minimum-perturbation potential,[5] this energy corresponds to a host potential chosen so that the atomic cell is electrically neutral, meaning that the perturbation will be confined to and screened within the impurity cell. Considering A_l to be a renormalization factor for the wave function inside the impurity muffin-tin cell, a value of unity therefore could be interpreted to imply that the host has little influence on the wave function inside the impurity cell.

In conclusion, we have proved an identity that allows band-structure calculations—in particular, phase-shift parametrizations—to be used directly to describe impurity scattering in terms of the scattering phase shifts of the impurity. To fit experimentally observed Dingle temperatures requires little or no more calculation than is often already available from the procedure of phase-shift parametrization. When fitted to a set of impurity phase shifts, the calculation automatically provides an inversion scheme for Dingle temperatures that gives not only the point scattering but also, with a little additional calculation, $P(k, k')$, the probability of scattering from a point k to k', required for calculating transport properties.

I wish to thank Dr. R. Harris, Dr. M. J. G. Lee, and Dr. M. Rasolt for helpful discussions, and Dr. I. M. Templeton for help and advice on many aspects of the computation.

[1]M. J. G. Lee, Phys. Rev. 178, 953 (1969); Phys. Rev. 187, 901 (1969).
[2]J. F. Cooke, H. L. Davis, and R. F. Wood, Phys. Rev. Letters 25, 28 (1970).
[3]N. J. Coenen and A. R. de Vroomen, J. Phys. F: Metal Phys. 2, 487 (1972).
[4]J. C. Shaw, J. B. Ketterson, and L. R. Windmiller, Phys. Rev. B 5, 3894 (1972).
[5]M. J. G. Lee and V. Heine, Phys. Rev. 5, 3839 (1972).
[6]For a review, see, M. Springford, Adv. in Physics 21, 4931 (1972).
[7]P. T. Coleridge, J. Phys. F: Metal Phys. 2, 1016 (1972).
[8]R. Harris, J. Phys. F: Metal Phys. 3, 89 (1973).
[9]G. J. Morgan, Proc. Phys. Soc. 89, 365 (1966).
[10]J. W. Blaker and R. Harris, J. Phys. C: Solid St. Phys. 4, 569 (1971).
[11]When differentiating with respect to one phase shift η_l, it is assumed that the others are kept constant.
[12]T. Loucks, *Augmented Plane Wave Method* (Benjamin, New York, 1967), p. 71.
[13]M. J. G. Lee, Phys. Rev. B 2, 250 (1970).

PHYSICAL REVIEW B VOLUME 7, NUMBER 8 15 APRIL 1973

Role of Bulk and Surface Plasmons in the Emission of Slow Secondary Electrons: Polycrystalline Aluminum*

Victor E. Henrich
Lincoln Laboratory, Massachusetts Institute of Technology, Lexington, Massachusetts 02173
(Received 26 July 1972)

Measurement of both the low-energy (true-secondary) and high-energy (characteristic-loss regions of the secondary-electron-emission spectrum of several types of polycrystalline aluminum have been made in order to explain structure seen at very low energies (0–20 eV). The data indicate that the structure is due to hot electrons losing energy by the creation of plasmons rather than by excitation of single electrons by decaying plasmons, as had been previously suggested.

I. INTRODUCTION

The strong coupling between electrons and plasmons has made electron-beam transmission and reflection experiments the major source of information on collective electron oscillations in solids. The most extensive work has been done by analyzing the energy of a beam of monochromatic high-energy electrons (primary energy E_p about 10–50 keV) after transmission through a thin solid sample.[1] In addition to the unscattered beam at energy E_p, peaks are found in the energy distribution curve (EDC) which are shifted to lower energy by the energy of one or more bulk plasmon $\hbar\omega_B$ or a surface plasmon $\hbar\omega_s$.[2] These are, of course, electrons that have created one or more plasmons in the material while passing through. Plasmon loss peaks have also been observed in the EDC's

of electrons reflected or scattered from bulk samples. In fact, inelastic low-energy-electron diffraction (ILEED) is currently the most productive tool for obtaining detailed information about plasma oscillations.[3] By analyzing not only the energy but also the momentum of the scattered electrons, it has been possible to determine the dispersion relation for surface plasmons.[4]

Once plasmons have been created in a material, several modes of decay are available to them.[1] The most probable mode, at least for long-wavelength plasmons, is through plasmon-phonon interactions. For short wavelengths in the vicinity of the plasmon cutoff wave number, it is possible for a plasmon to excite a single electron. Other competing modes are radiative decay[5] and creation of an exciton.

Two years ago, von Koch[6] reported the observation of peaks in the low-energy region of the secondary-electron spectrum of aluminum and several other materials which were attributed to the excitation of a single electron by a decaying plasmon. The peaks occurred at an absolute kinetic energy equal to the plasmon energy (not shifted down by the sample work function), and both bulk and surface plasmons were reported. No special properties of the samples were given, and no restrictions on the momentum of the analyzed electrons were mentioned.

In the course of studies of the secondary-emission characteristics of a variety of metals, semiconductors and insulators, we have never observed such large amplitude structure in the low-energy region. In general, the slow-electron spectrum below about 50 eV consists of the large, smooth, "true" secondary peak, with the only structure being Auger peaks. Some additional weak structure is seen in heavy elements like gold and silver.[7] and carefully prepared single-crystal surfaces have shown structure due either to diffraction effects[7] or to concentration of electrons at regions of high density of states in the excited conduction bands.[8]

We report here detailed studies of the shape of the slow-secondary-electron spectrum from samples of polycrystalline aluminum that are in distinct disagreement with the results of von Koch.[6] Only weak structure is observed, and it occurs at the energies predicted by theory.[9] By using polycrystalline rather than single-crystal samples and by collecting the electrons emitted at all angles, diffraction effects are not present and band-structure effects should be minimized. (Measurements on other materials will be discussed in Sec. VI.) The data indicate that plasmons enter as possible loss channels for hot secondary electrons[9] rather than as sources for them. The effects of both bulk and surface plasmons can be seen.

II. PLASMON-ELECTRON INTERACTIONS

When a beam of electrons is incident on a solid, the electrons can excite one or more plasmons before being transmitted or diffracted out of the material. These electrons emerge with energy $E_p - n_B\hbar\omega_B - n_s\hbar\omega_s$, where n_B and n_s are the number of bulk and surface plasmons created, and these peaks constitute part of the characteristic energy-loss region of the secondary-electron spectrum just below the elastically reflected primary beam. For materials like aluminum with very strong electron-plasmon coupling, these plasmon-loss peaks make up the bulk of the structure in this region.

The spectra of slow, "true" secondary electrons ($E < 50$ eV) emitted from a sample under bombardment by higher-energy primaries constitute quite a different picture. Excluding Auger electrons, these slow secondaries consist of hot electrons generated in the bulk of the sample that have diffused to the surface, losing energy on the way. ("Bulk" may mean only tens of angstroms in from the surface, depending on primary-energy and secondary-electron diffusion lengths.) In the simplest terms, the energy distribution of these electrons, $n(E)$, is a product of the hot-electron energy distribution just inside the sample surface, $n_H(E)$, and the escape probability for these electrons.[7,10,11] The latter is a smooth function of the form[11]

$$P(E) = 1 - [(\varphi + E_F)/E]^{1/2},$$

where E is the hot-electron energy, E_F is the Fermi energy, and φ is the sample work function. (Energy is measured from the bottom of the conduction band in this expression.) $P(E)$ goes from zero at the vacuum level to unity a few volts above it and is responsible for the peak in $n(E)$ at 2–5 eV. Any additional structure in $n(E)$ is due to structure in $n_H(E)$. The shape of $n_H(E)$ is determined by the various loss channels available to hot electrons as well as secondary-electron generation, elastic scattering and diffraction of hot electrons, etc. It has the same general shape for all materials, however, increasing rapidly as the hot-electron energy approaches the Fermi level.[7,9–11]

If plasmon creation is available as a loss mechanism for hot electrons, then one can make some qualitative statements about its effect on $n_H(E)$.[9] Consider the band diagram in Fig. 1. Here φ is the work function of the sample, and the energy scale on the right-hand side is absolute kinetic energy measured in vacuum. Electrons with energies above the dashed line at $E_F + \hbar\omega_B$ have all loss channels available to them. They can create bulk or surface plasmons (for a clean surface, $\hbar\omega_s = \hbar\omega_B/\sqrt{2}$) or lose energy by scattering from conduction electrons, phonons, excitons, etc. Once they have dropped below $E_F + \hbar\omega_B$, however, they

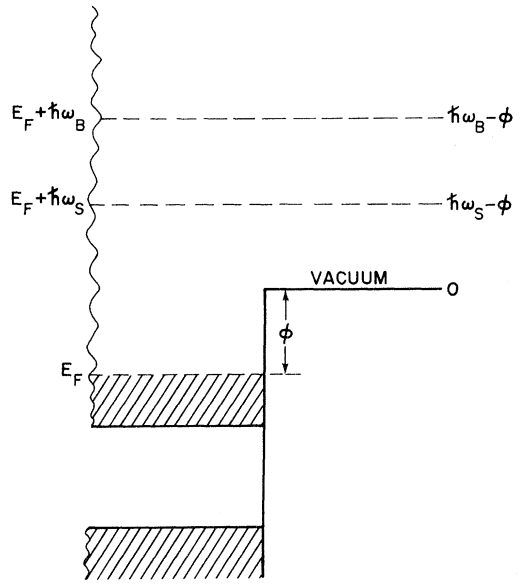

FIG. 1. Energy diagram showing limits of plasmon-loss modes. The energy scale on the right-hand side is kinetic energy measured in vacuum.

can no longer create a bulk plasmon; there are no available final states for the electron. Similarly, once they have dropped below $E_F+\hbar\omega_s$, surface-plasmon creation is no longer a possible process.

Assuming that all nonplasmon loss processes give a smoothly varying contribution to $n_H(E)$ in this energy range,[10,11] we can see the effects of the closing of plasmon-loss channels on $n_H(E)$. Above $E_F+\hbar\omega_B$, where both plasmon-loss modes are available, the rate of energy loss of the hot electron will be very large. Due to the dependence of energy-loss rate on electron energy, this gives an $n_H(E)$ which increases rapidly with decreasing E.[9] Between $E_F+\hbar\omega_s$ and $E_F+\hbar\omega_B$, $n_H(E)$ will increase more slowly with decreasing E, and below $E_F+\hbar\omega_s$ the rate of change of $n_H(E)$ will be still smaller. This is sketched in Fig. 2. The resultant $n_H(E)$, and hence $n(E)$, will have discontinuities in slope at kinetic energies of $\hbar\omega_B-\varphi$ and $\hbar\omega_s-\varphi$, measured in vacuum.

We should note that in the alternative process of excitation of a single electron by a decaying plasmon, considered by von Koch,[6] the electron would come from the Fermi level or below, not the vacuum level, and would hence have a kinetic energy after escape no greater than $\hbar\omega_B-\varphi$ rather than $\hbar\omega_B$.

The problem of coupling of hot electrons of all energies to plasmons is sufficiently complicated[3] that it is not possible to make quantitative statements about the size of the effects to be expected here. Empirically, the largest effects are seen in free-electron-like metals (see Sec. VI). Also, the electron-plasmon coupling is different enough from the photon-plasmon coupling that one cannot extrapolate from photon scattering experiments. In silver, for example, surface plasmons have been observed by light scattering,[12] and yet no structure due to either surface or bulk plasmons is seen in low-energy-electron scattering experiments.

III. EXPERIMENT

A. Samples

Three types of polycrystalline aluminum samples were used in this experiment. One was a 0.012-in. rolled sheet whose surface was not treated or polished before use. X-ray fluorescent analysis showed the major impurities to be (be weight) 0.5% Fe, 0.1% Cu, 0.03% Ga, and 0.01% Cr. The second sample was ordinary 0.0015-in. heavy-duty aluminum foil, on which spectrophotometry, x-ray fluorescence, and mass spectrometry yielded an impurity content (by weight) of 0.84% Fe, 0.05% Na, and 0.03% Zn. The highly reflecting side was used, and care was taken to maintain the surface as flat as possible. The last sample was a pellet of Gallard–Schlesinger 40/200-mesh 99.995+%-pure aluminum powder pressed in a highly polished stainless-steel die at 200 kpsi. Mass spectrometry showed its impurities to be (by weight) 290 ppm Si, 190 ppm C, and 140 ppm Fe. The pellet was dense with a reflecting surface, but not as highly reflecting as the foil. These samples were chosen

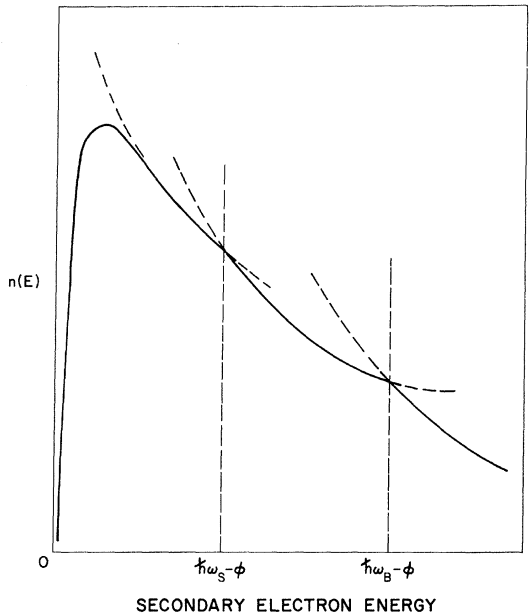

FIG. 2. Effect of plasmon losses on the secondary-electron energy distribution $n(E)$.

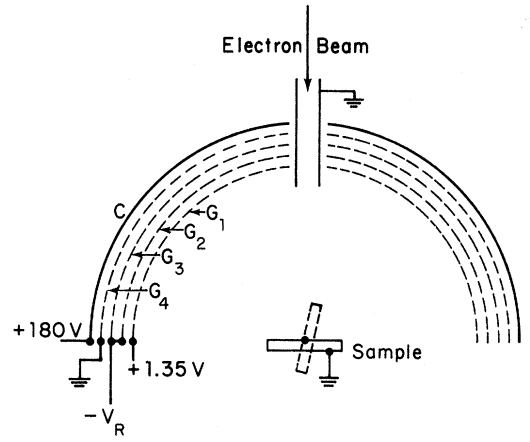

FIG. 3. Spherical retarding grid analyzer used to measure secondary-electron spectra. The dashed rectangle shows the sample position for grazing incidence.

to give a diversity of impurity content and surface structure. All samples were ultrasonically cleaned in acetone followed by ethanol before mounting in the vacuum chamber. The entire vacuum system was then baked at 250 °C for 12–24 at a pressure below 2×10^{-8} Torr before any measurements were made. Final cleaning was done by argon-ion sputtering, which will be discussed later.

B. Experimental Apparatus

All measurements were made on a Physical Electronics Industries, Inc. LEED/Auger spectrometer with a four-grid, 180° spherical regarding-grid analyzer and coaxial electron gun (Fig. 3). For all measurements reported here, the electron gun was run at 1000 V with a beam current of about 10 μA and a current density near 10 mA/cm^2. The sample was grounded, as was the last anode of the electron gun, and G_1 was biased at +1.35 V to provide a nearly field-free region around the sample and yet eliminate space-charge problems for very-low-energy electrons. G_2 and G_3 were biased with the retarding voltage V_R and modulation was also applied to them for derivative detection. G_4 was grounded to prevent capacitive pickup of the modulating signal by the collector C, and C was maintained at +180 V to suppress secondary emission from the collector.

The work functions of the sample and the analyzing grids must be taken into account in determining the absolute energy of emitted electrons. Since the sample and analyzing grids are referenced at their Fermi levels, zero retarding voltage on the grids corresponds to an energy φ_{grid} above the sample Fermi level (here the grids are chromium plated, so $\varphi_{\text{grid}}\approx 4.6$ eV). To convert measured voltages to energy above the aluminum Fermi level, we just add 4.6 eV. The low-voltage cutoff in $n(E)$ is determined by the sample vacuum level, however, which occurs at a retarding voltage of $\varphi_{\text{Al}}-\varphi_{\text{grid}}$, or about +0.5 V.

For some measurements, a sample holder was used which permitted the sample to be rotated about an axis tangent to its surface in order to change the angle of incidence of the electron beam (see Fig. 3). Since the secondary electrons measured were those reaching the collector, not all of them were collected unless the sample surface was normal to the electron beam. At grazing incidence only about half of the electrons are collected (recall that the angular distribution of true secondaries is almost independent of the angle of incidence), so it was not possible to make quantitative comparisons of secondary-electron intensity at different angles. The shape of the secondary-electron spectra was not affected, however, so accurate relative measurements could be made.

The vacuum system employed liquid-nitrogen-cooled sorption roughing pumps with ion and titanium sublimation pumps for ultrahigh vacuum. Measurements were made at a total system pressure of $<5\times10^{-10}$ Torr and a partial pressure of all gases other than argon of $<2\times10^{-10}$ Torr. The samples were cleaned by sputtering with 500-eV argon ions at a current density of about 15 μA/cm^2. The sputtering time varied, as mentioned below. The state of the sample surface was monitored by Auger spectroscopy. After the initial pumpdown and system bakeout, strong carbon and oxygen Auger lines were observed. An additional 2 h of sputtering removed all traces of both elements.

IV. PLASMON STRUCTURE IN INELASTIC PRIMARY SPECTRA

Plasmon-loss peaks are always observed in the characteristic-loss region of clean aluminum samples. An example of this structure for normal beam incidence in a clean sample of aluminum foil is shown in the top trace in Fig. 4, where $n(E)$ is plotted versus secondary-electron energy. The periodic series of peaks spaced by about 15 eV are multiple bulk-plasmon losses. In some samples, we have seen as many as ten of these loss peaks, extending to 150 eV below the elastic peak. It is this very strong plasmon coupling which gives aluminum observable structure in the slow secondary spectra.

The smaller peak about 10 eV below the elastic peak (indicated by the arrow) has the proper energy to be the surface plasmon.[4] Since its unambiguous identification is necessary to interpret slow-electron data, however, we studied its behavior as a function of angle incidence of the primary beam. Due to the large solid angle of collection used here

we are averaging over all momenta and should see no shift in energy of this peak as the angle of incidence is varied. The amplitude of the surface-plasmon peak relative to that of the bulk plasmon should increase with decreasing angle of incidence (measured to the sample surface), however, just due to the shallower penetration depth of the primary beam. The remaining traces in Fig. 4 show the spectra for angles of incidence of 20°, 10°, and 5°. The 10-eV peak grows in intensity until at 5° it dominates the bulk-plasmon-loss peak, clearly indicating its surface nature. The same behavior was seen in the pressed pellet after thorough cleaning.

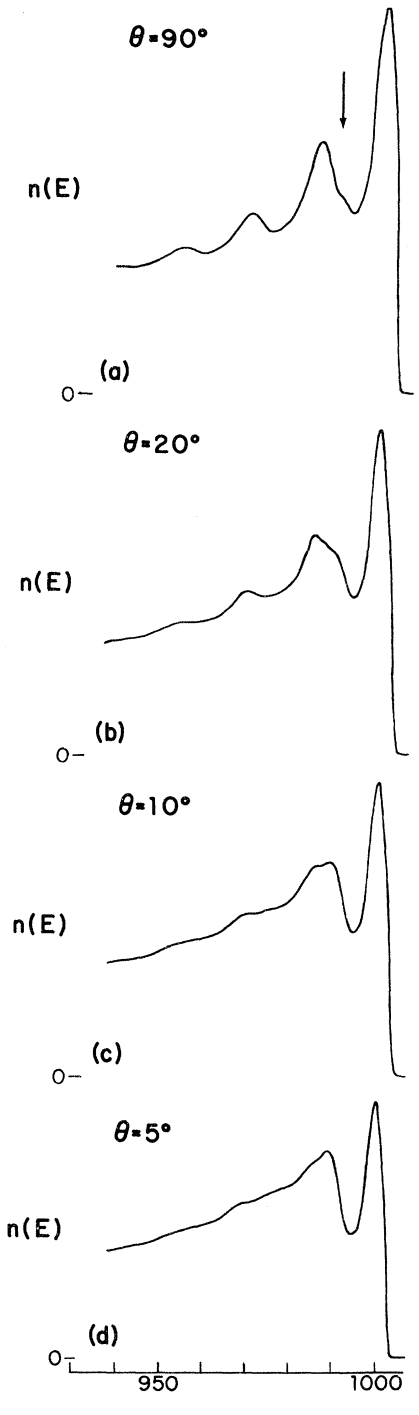

FIG. 4. Characteristic energy-loss spectra for aluminum foil for various angles of primary beam incidence. θ is the angle between the primary beam and the sample surface.

While strong bulk-plasmon structure was seen in all aluminum samples, the surface-plasmon-loss peak varies considerably in intensity depending on the state of cleanliness of the surface. (Comparative measurements were made with the primary beam always normal to the surface.) It was always present on very clean surfaces (sputtered 2 h or more). Trace amounts of carbon and oxygen on the surface, however, correlated with reduced intensity or total absence of the peak. It is important to note that by "trace amounts" we mean amounts small compared to those present before any sputtering. Most samples have such "dirty" surfaces after pumpdown that not even the bulk-plasmon-loss peaks can be seen clearly. After 1 h of sputtering only very small carbon and oxygen Auger peaks remain and the bulk-plasmon losses are strong. The varying strength of the surface-plasmon peak is thus not due to attenuation of the electrons in some surface coating, but arises from the effect of small amounts of adsorbed material on the electron-plasmon coupling.[13]

V. SLOW-ELECTRON SPECTRA

The spectrum of slow electrons emitted from aluminum looks qualitatively like the spectra for virtually all other materials (excluding Auger peaks or single-crystal effects mentioned in Sec. I): a large peak at 2–5 eV with a rapid decrease in $n(E)$ at higher energies. Typical $n(E)$ curves for aluminum are shown on the left-hand side of Fig. 5. No additional peaks in $n(E)$ are seen, with the only visible structure being a slight break in the curve at about 10.5 V. Because of the lack of much detail in $n(E)$, the derivative of $n(E)$ with respect to electron kinetic energy, $-dn(E)/dE$, was also recorded, and we will in general discuss its structure in interpreting the shape of $n(E)$. This derivative is shown in the middle of Fig. 5. The high-energy characteristic-loss spectrum was also measured and is presented on the right-hand side of Fig. 5. The vertical scale for the low-energy region of $n(E)$ has been attenuated by a factor of 50 relative to that for the high-energy spectra, so that almost all of the electrons emitted by the sample are at very low energy.

Figure 5 presents data on the high-purity

pressed pellet for normal-incidence primary electrons at different stages of surface treatment. In Fig. 5(a), the sample had been sputtered for 1 h, and only very small carbon and oxygen Auger peaks were present. While the bulk-plasmon structure at high energies is very large, there is no trace of the surface plasmon. The only structure in the low-energy $n(E)$ here is one change in slope at 10.5 eV, which is more easily seen in $dn(E)/dE$. Adding the grid work function, this is 15.1 eV above the aluminum Fermi level, and we believe it corresponds to the change in slope of $n_H(E)$ when bulk-plasmon excitation is no longer a possible loss mechanism for hot electrons.

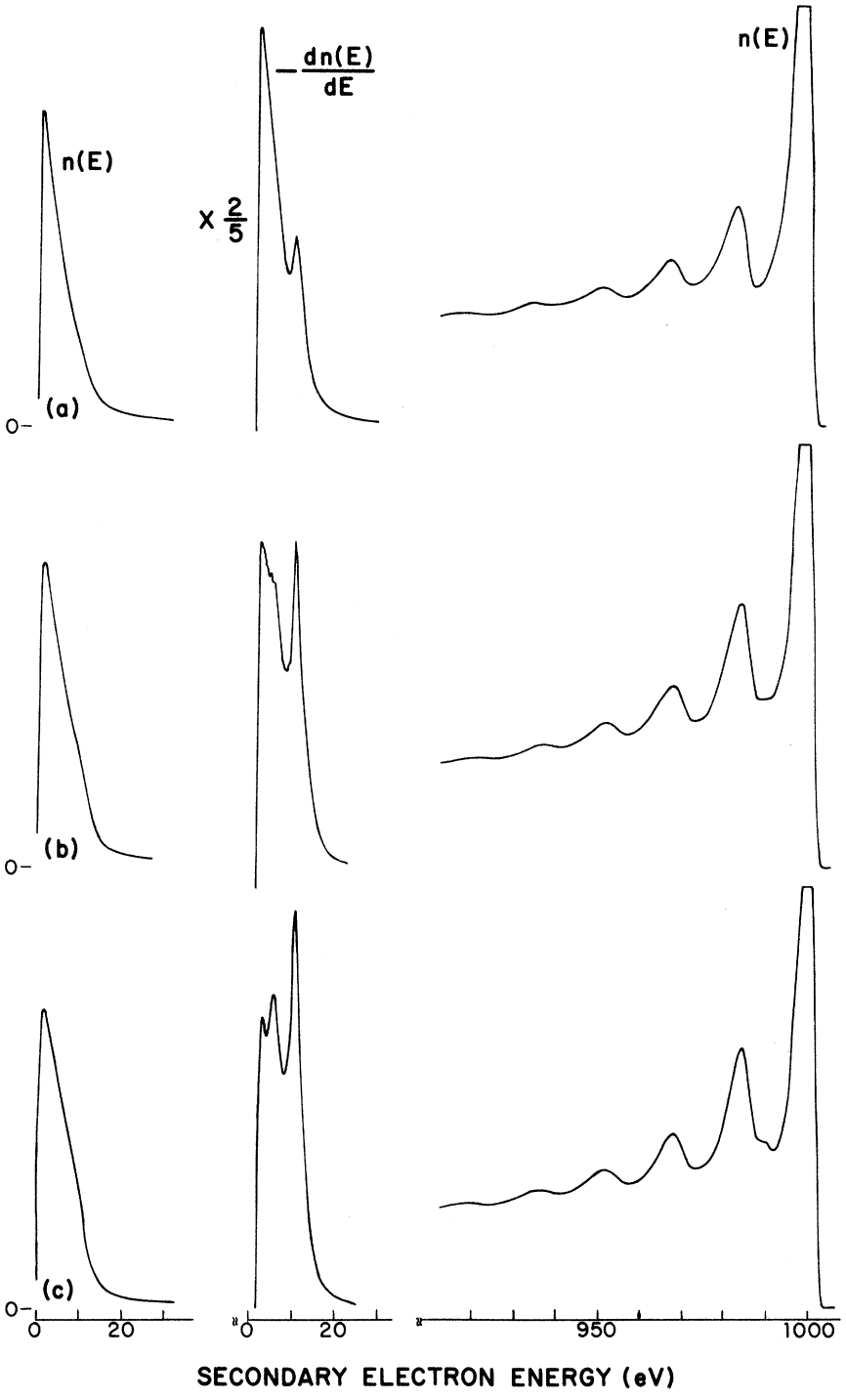

FIG. 5. Secondary-electron spectra for various surface conditions of the pressed aluminum pellet (see text for details). Abscissa is electron kinetic energy in vacuum. Modulation amplitude: 0.2 V peak to peak for low-energy $n(E)$, 1.0 V peak to peak for $dn(E)/dE$ and high-energy $n(E)$.

Figure 5(b) shows the same sample after it was thoroughly cleaned and then allowed to remain in a vacuum of about 1.3×10^{-10} Torr for two weeks. An Auger trace showed a weak carbon peak but no detectable oxygen lines. The high-energy loss spectrum shows different detail in the region of the surface plasmon—no distinct peak, but $n(E)$ is much flatter there. The different slow-electron structure is obvious from $dn(E)dE$. In addition to relative changes in amplitude, weak detail (above the noise) exists near 5 eV. Further sputtering of the sample until no trace of any surface contamination existed yielded the results in Fig. 5(c). The surface-plasmon peak is now clearly visible

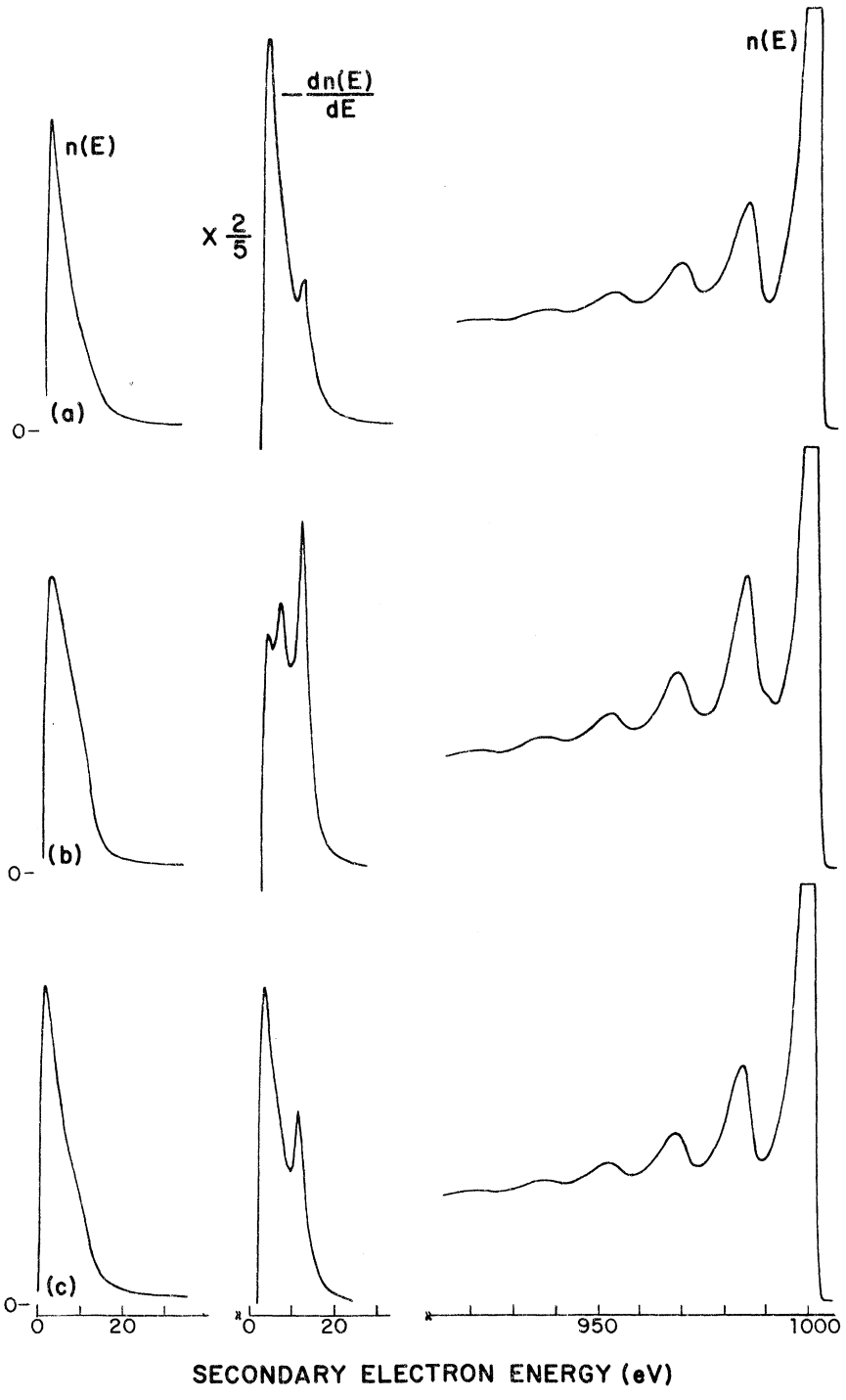

FIG. 6. Secondary-electron spectra for aluminum foil [(a) and (b)] and aluminum sheet [(c)]. Modulation is the same as in Fig. 5.

in the high-energy data, and a second discontinuity in slope has appeared in the low-energy $n(E)$, although it can only be seen clearly in $dn(E)/dE$. Its location at 5.5 V, or 10.1 eV above the aluminum Fermi level, is very close to the surface-plasmon energy. We believe that it arises from the closing of the surface-plasmon-loss channel.

Figure 6 shows the same type of data for two other samples. Figure 6(a) shows an aluminum-foil sample after about 1 h of sputtering, where traces of carbon and oxygen remained on the surface. As above, there is no trace of a surface-plasmon-loss peak at high energies, and only one discontinuity in slope occurs in $n(E)$ at low energies. After the foil was thoroughly sputtered [Fig. 6(b)], the surface peak appears in the characteristic-loss spectrum as does the second slope change at about 5.5 V. Figure 6(c) shows the sample of aluminum sheet after thorough cleaning followed by a two-week storage at 1.3×10^{-10} Torr. Again no surface-plasmon effects are present at either end of the spectrum. (Unfortunately, further measurements on the sheet sample were not made.)

VI. DISCUSSION

We believe that the above data correlating the effects of bulk and surface plasmons on high- and low-energy ends of the secondary-electron spectrum indicate that the role played by plasmons in the true-secondary region is one of an energy-loss mechanism for hot electrons diffusing toward the surface rather than as a source for single-electron excitation. We know of no aluminum Auger peak near 10.5 eV, and the peak at 5.5 eV could not be an Auger peak due to its extreme sensitivity to surface conditions. The large difference in impurity content of the three samples rules out the possibility of impurity Auger peaks.

We have looked for the effects of plasmons on secondary-electron emission in other materials, but in no case was the interpretation as unambiguous as for aluminum. The main limitation is the strength of the plasmon coupling to low-energy electrons. While most materials exhibit plasma losses in high-energy-electron transmission experiments, very few have clearly identifiable plasmon peaks in the characteristic-loss spectrum for low-energy incident electrons. All materials have some structure in the characteristic-loss region below the elastic peak, but much of it is due to band-structure effects rather than to plasmons. Materials such as silver, gold, copper, nickel, and platinum have peaks in this region, but the energies do not correspond to plasma losses, and peaks at multiples of the main loss peak do not occur. Structure is also observed in the slow-electron spectra of these materials, but again the energies do not correspond to plasma excitations, and they are believed to be due to band-structure effects, Auger transitions, and surface excited states.[7]

The only materials in which we have seen multiple plasmon characteristic-loss peaks (clearly indicating a strong plasmon-electron coupling at low energies) are aluminum, magnesium, silicon, germanium, and molybdenum. In magnesium, a change in slope of $n(E)$ occurs at the energy corresponding to the bulk plasmon, but we could not obtain a sufficiently oxide-free surface to get meaningful results. Silicon and germanium both have weak structure in $dn(E)/dE$ at their respective bulk-plasmon energies, but there is no evidence of surface-plasmon coupling, so nothing could be varied to uniquely identify the origin of the structure. Molybdenum has an Auger electron peak so close to the plasma energy that it masks any plasmon effects.

ACKNOWLEDGMENTS

The author would like to thank G. F. Dresselhaus, J. G. Mavroides, and H. J. Zeiger for many helpful discussion, J. A. Kafalas and E. B. Owens for help in sample preparation and analysis, and B. Feldman for assistance in taking the data.

*Work was sponsored by the U. S. Department of the Air Force.

[1]For a good review, see K. D. Sevier, *Low Energy Electron Spectrometry* (Interscience, New York, 1972), Chap. 8.

[2]For the properties of surface plasmons, see E. A. Stern and R. A. Ferrell, Phys. Rev. 120, 130 (1960), and references therein.

[3]C. B. Duke and G. E. Laramore, Phys. Rev. B 3, 3183 (1971); G. E. Laramore and C. B. Duke, Phys. Rev. B 3, 3198 (1971).

[4]A. Bagchi and C. B. Duke, Phys. Rev. B 5, 2784 (1972).

[5]A. J. Braundmeier, Jr., M. W. Williams, E. T. Arakawa, and R. H. Ritchie, Phys. Rev. B 5, 2754 (1972).

[6]C. V. von Koch, Phys. Rev. Letters 25, 792 (1970).

[7]M. P. Seah, Surface Science 17, 132 (1969).

[8]R. F. Willis, B. Feuerbacher, and B. Fitton, Phys. Rev. B 4, 2441 (1971).

[9]J. J. Quinn, Phys. Rev. 126, 1453 (1962).

[10]O. Hachenberg and W. Brauer, in *Advances in Electronics and Electron Physics*, edited by L. Marton (Academic, New York, 1959).

[11]P. A. Wolff, Phys. Rev. 95, 56 (1954).

[12]S. N. Jasperson and S. E. Schnatterly, Phys. Rev. 188, 759 (1969).

[13]Similar effects have been seen in GaAs: A. Y. Mityagin, V. P. Orlov and N. Y. Cherevatskii, Fiz. Tverd. Tela 13, 2159 (1971). [Soviet Physics-Solid State 13, 1815 (1972)].